

RECEIVER-COORDINATED ZERO-FORCING DISTRIBUTED TRANSMIT NULLFORMING

D. Richard Brown III*

Patrick Bidigare†

Soura Dasgupta‡

Upamanyu Madhow◇

* Worcester Polytechnic Institute, 100 Institute Road, Worcester, MA 01609, drb@wpi.edu

† Raytheon BBN Technologies, 1300 17th Street Suite 400, Arlington, VA 22207, bidigare@ieee.org

‡ University of Iowa, Iowa City, IA 52242, dasgupta@engineering.uiowa.edu

◇ University of California, Santa Barbara, CA 93106, madhow@ece.ucsb.edu

ABSTRACT

A coherent cooperative communication system is proposed in which a distributed array of transmit nodes forms a beam at a desired receiver while simultaneously steering nulls at several protected receivers. Coherent transmission is achieved through a receiver-coordinated protocol where the receivers in the system use state-space channel tracking and provide feedback to the transmit cluster to facilitate distributed transmission. Analytical estimates for the performance degradation in the nulls due to channel estimation errors are verified by simulations. Numerical results demonstrate that the technique is effective even with low channel measurement overhead, infrequent measurement intervals, and feedback latency.

Index Terms— cooperative communication, distributed transmission, feedback systems, oscillator dynamics, tracking

1. INTRODUCTION

Coherent cooperative transmission is a technique in which $N \geq 2$ transmitters control the phase and amplitude of their transmissions to form a virtual (and typically sparse) antenna array. Distributed beamforming, see e.g. [1], is one example of this technique. In this paper, we develop and analyze a coherent cooperative transmission system which simultaneously performs distributed beamforming to one intended receiver and distributed *nullforming* to M protected receivers. Each receiver tracks, using a state space model, a time-varying state of “effective” channel phase and frequency offsets which include stochastic clock drift. Explicit state feedback from the $M+1$ total receivers is then used by each transmit node to predict the $N \times (M+1)$ channel matrix and compute a “zero-forcing” transmit vector \mathbf{w} for use during distributed transmission.

This paper demonstrates the efficacy of this receiver-coordinated zero-forcing distributed transmit nullforming technique in the face of channel time variations caused by stochastic local oscillator drift. Unlike the prior work in [2, 3], we do not assume the transmit cluster is synchronized and the approach here is simplified in that the calculation of the transmit vector does not require knowledge of the state prediction error covariance. We also provide analytical performance estimates, verified using simulations, of the nullforming performance degradation due to channel estimation errors.

2. SYSTEM MODEL

We consider a wireless communication system with N transmit nodes, M protected receivers, and one intended receiver. Each node in the system is assumed to possess a single antenna. We also assume the transmit nodes have some mechanism by which they can share a common baseband message to be transmitted to the

intended receiver and also have some rough level of synchronization so that they can effectively participate in the receiver-coordinated protocol schedule described in Section 3. The coarse synchronization required here can be achieved with standard techniques such as global positioning system (GPS), network time protocol (NTP), or potentially through feedback messages from the receive nodes. Precise carrier synchronization as described in [4] is not assumed, but is implicitly achieved via channel tracking and feedback. The nominal transmit frequency in the forward link from the distributed transmit cluster to the receivers is at ω_c . All forward link channels are modeled as narrowband, linear, and time invariant (LTI). Enumerating the protected receivers as $m = 1, \dots, M$ and adopting the convention that the intended receiver is node 0, we denote the channel from transmit node n to receive node m at carrier frequency ω_c as $g_{n,m} \in \mathbb{C}$ for $n = 1, \dots, N$ and $m = 0, \dots, M$. These LTI propagation channels, in contrast to the time-varying “effective” channels described below, do not include the effect of carrier phase offsets between transmit node n and receive node m .

The receiver-coordinated protocol requires all of the receivers in the system to measure and track the channels from the transmit cluster and to provide feedback to the transmit cluster to facilitate distributed transmission. Figure 1 shows the effective narrowband channel model from transmit node n to receive node m which includes the effects of propagation, transmit and receive gains, and carrier offset. Transmissions $n \rightarrow m$ are conveyed on a carrier nominally at ω_c generated at transmit node n , incur a phase shift of $\psi^{(n,m)} = \angle g_{n,m}$ over the wireless channel, and are then down-mixed by receive node m using its local carrier nominally at ω_c . At time t , the effective narrowband channel from transmit node n to receive node m is modeled as

$$h^{(n,m)}(\tau) = g_{n,m} e^{j(\phi_t^{(n)}(\tau) - \phi_r^{(m)}(\tau))} = |g_{n,m}| e^{j\phi^{(n,m)}(\tau)} \quad (1)$$

where $\phi_t^{(n)}(\tau)$ and $\phi_r^{(m)}(\tau)$ are the local carrier phase offsets at transmit node n and receive node m , respectively, at time τ with respect to an ideal carrier reference, and $\phi^{(n,m)}(\tau) = \phi_t^{(n)}(\tau) - \phi_r^{(m)}(\tau) + \psi^{(n,m)}$ is the pairwise phase offset after propagation between transmit node n and receive node m at time τ .

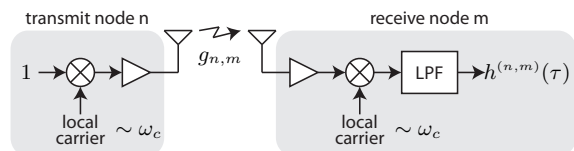


Fig. 1. Effective narrowband channel model including the effects of propagation, transmit and receive gains, and carrier offset.

2.1. Dynamic Local Carrier Phase Offset Model

Each transmit and receive node in the system is assumed to have an independent local oscillator. These local oscillators have inherent frequency offsets and behave stochastically, causing phase offset variations in each “effective” channel from transmit node n to receive node m even when the propagation channels $g_{n,m}$ are otherwise time invariant. This section develops a discrete-time state-space model to characterize the dynamics of the phase variations and facilitate channel tracking for efficient distributed transmission.

Based on the two-state models in [5], we define the discrete-time state of the n^{th} transmit node’s carrier as

$$\mathbf{x}_t^{(n)}[k] = [\phi_t^{(n)}[k], \dot{\phi}_t^{(n)}[k]]^\top$$

where $\phi_t^{(n)}[k]$ corresponds to the carrier phase offset in radians at transmit node n with respect to an ideal carrier phase reference. The state update of the n^{th} transmit node’s carrier is governed by

$$\mathbf{x}_t^{(n)}[k+1] = \mathbf{f}(T_s)\mathbf{x}_t^{(n)}[k] + \mathbf{u}_t^{(n)}[k] \text{ with } \mathbf{f}(T_s) = \begin{bmatrix} 1 & T_s \\ 0 & 1 \end{bmatrix} \quad (2)$$

where T_s is an arbitrary sampling period selected to be small enough to avoid phase aliasing at the largest expected frequency offsets. The process noise vector $\mathbf{u}_t^{(n)}[k] \stackrel{\text{i.i.d.}}{\sim} \mathcal{N}(\mathbf{0}, \mathbf{Q}_t^{(n)}(T_s))$ corresponds to the white frequency and random walk frequency process noises that cause the carrier derived from the local oscillator at transmit node n to deviate from an ideal linear phase trajectory. The covariance of the discrete-time process noise is derived from a continuous-time model in [5] and is given as

$$\mathbf{Q}_t^{(n)}(T_s) = \omega_c^2 T_s \begin{bmatrix} p_t^{(n)} + q_t^{(n)} \frac{T_s^2}{3} & q_t^{(n)} \frac{T_s}{2} \\ q_t^{(n)} \frac{T_s}{2} & q_t^{(n)} \end{bmatrix} \quad (3)$$

where ω_c is the nominal common carrier frequency in radians per second and $p_t^{(n)}$ (units of seconds) and $q_t^{(n)}$ (units of Hertz) are the process noise parameters corresponding to white frequency noise and random walk frequency noise, respectively. The process noise parameters $p_t^{(n)}$ and $q_t^{(n)}$ can be estimated by fitting the theoretical Allan variance $\sigma_y^2(\tau) = p_t^{(n)}/\tau + q_t^{(n)}\tau/3$ to experimental measurements of the Allan variance over a range of τ values.

The receive nodes in the system also have independent local oscillators used to generate carriers for downmixing that are governed by the same dynamics as (2) with state $\mathbf{x}_r^{(m)}[k]$, process noise $\mathbf{u}_r^{(m)}[k] \stackrel{\text{i.i.d.}}{\sim} \mathcal{N}(\mathbf{0}, \mathbf{Q}_r^{(m)}(T_s))$, and process noise parameters $p_r^{(m)}$ and $q_r^{(m)}$ as in (3) for $m = 0, \dots, M$.

2.2. Dynamic Pairwise Carrier Phase Offsets

The *pairwise offset* after propagation is defined as

$$\delta^{(n,m)}[k] = \begin{bmatrix} \phi^{(n,m)}[k] \\ \dot{\phi}^{(n,m)}[k] \end{bmatrix} = \mathbf{x}_t^{(n)}[k] + \begin{bmatrix} \psi^{(n,m)} \\ 0 \end{bmatrix} - \mathbf{x}_r^{(m)}[k]$$

and is governed by the state update

$$\delta^{(n,m)}[k+1] = \mathbf{f}(T_s)\delta^{(n,m)}[k] + \mathbf{u}_t^{(n)}[k] - \mathbf{u}_r^{(m)}[k]. \quad (4)$$

At receiver m , the $2N$ -dimensional vector state of pairwise carrier offsets $\Delta^{(m)}[k] = [(\delta^{(1,m)}[k])^\top, \dots, (\delta^{(N,m)}[k])^\top]^\top$ is then

$$\begin{aligned} \Delta^{(m)}[k+1] &= \begin{bmatrix} \mathbf{f}(T_s) & & \\ & \ddots & \\ & & \mathbf{f}(T_s) \end{bmatrix} \Delta^{(m)}[k] + \begin{bmatrix} \mathbf{u}_t^{(1)}[k] - \mathbf{u}_r^{(m)}[k] \\ \vdots \\ \mathbf{u}_t^{(N)}[k] - \mathbf{u}_r^{(m)}[k] \end{bmatrix} \\ &= \mathbf{F}(T_s)\Delta^{(m)}[k] + \mathbf{z}^{(m)}[k]. \end{aligned}$$

Note the process noise $\mathbf{z}^{(m)}[k] = \mathbf{G}\mathbf{u}^{(m)}[k]$ where

$$\mathbf{G} = \begin{bmatrix} \mathbf{I}_2 & & & -\mathbf{I}_2 \\ & \ddots & & \vdots \\ & & \mathbf{I}_2 & -\mathbf{I}_2 \end{bmatrix} \text{ and } \mathbf{u}^{(m)}[k] = \begin{bmatrix} \mathbf{u}_t^{(1)}[k] \\ \vdots \\ \mathbf{u}_t^{(N)}[k] \\ \mathbf{u}_r^{(m)}[k] \end{bmatrix}$$

and where \mathbf{I}_2 is the 2×2 identity matrix. Under the assumption that the constituent clock process noises are all independent such that

$$\begin{aligned} \text{cov}\{\mathbf{u}^{(m)}[k]\} &= \text{blockdiag}\{\mathbf{Q}_t^{(1)}(T_s), \dots, \mathbf{Q}_t^{(N)}(T_s), \mathbf{Q}_r^{(m)}(T_s)\} \\ &= \mathbf{Q}^{(m)}(T_s) \end{aligned}$$

we can say the $2N$ -dimensional vector process noise at receiver m is distributed as $\mathbf{z}^{(m)}[k] \sim \mathcal{N}(\mathbf{0}, \mathbf{G}\mathbf{Q}^{(m)}(T_s)\mathbf{G}^\top)$.

3. RECEIVER-COORDINATED PROTOCOL

An overview of the receiver-coordinated distributed transmission protocol is shown in Figure 2; see [3] for a more detailed description. Forward transmissions are divided into measurement and distributed transmission epochs, repeating periodically with period T_m which corresponds to the measurement interval. Reverse link transmissions provide feedback from the receive nodes to the transmit nodes and are assumed to be on a different channel than the forward link signals. Note that the protocol includes the effects of feedback latency since the feedback is typically not incorporated in the transmit weights until a later distributed transmission interval.

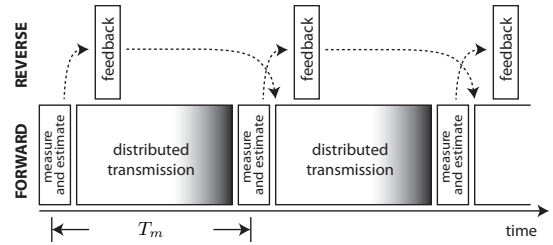


Fig. 2. Receiver-coordinated distributed transmission.

The duration of the measurement epoch is assumed to be small with respect to the frequency offsets such that the phase of the received signal is approximately constant during measurements. At time k , receive node m directly downmixes the received carrier from transmit node n with its own local carrier and estimates the resulting phase offset according to the observation model

$$\mathbf{y}^{(m)}[k] = \begin{bmatrix} 1 & 0 & & \\ & \ddots & \ddots & \\ & & & 1 & 0 \end{bmatrix} \Delta^{(m)}[k] + \begin{bmatrix} v^{(1,m)}[k] \\ \vdots \\ v^{(N,m)}[k] \end{bmatrix} \quad (5)$$

$$= \mathbf{H}\Delta^{(m)}[k] + \mathbf{v}^{(m)}[k] \quad (6)$$

where $\mathbf{v}^{(m)}[k] \stackrel{\text{i.i.d.}}{\sim} \mathcal{N}(\mathbf{0}, \mathbf{R}^{(m)})$ is the additive white Gaussian measurement noise in the observation with $\mathbf{R} = \text{diag}(r_{1,m}, \dots, r_{N,m})$.

Since the pairwise offset states are coupled across receive nodes, the optimal approach to tracking the states is to feed the $M+1$ measurement vectors (6) back to the transmit nodes and have each transmit node apply the overall measurement vector to a Kalman filter to generate the joint MMSE state estimate $\hat{\Delta}[k|k] \in \mathbb{R}^{2N(M+1)}$. This

approach, however, places the computational burden on the transmit nodes and also results in redundant computation. We propose instead a suboptimal (but more scalable) approach in which each receive node applies its observation vector $\mathbf{y}^{(m)}[k]$ to a Kalman filter to generate a local MMSE state estimate $\hat{\Delta}^{(m)}[k|k] \in \mathbb{R}^{2N}$. These state estimates are then fed back to the transmit cluster to facilitate distributed transmission.

Once the transmit cluster has received the feedback, the phase of the effective channels at any time $\ell > k$ can be straightforwardly predicted. Denoting the MMSE phase prediction as $\hat{\phi}^{(n,m)}[\ell|k]$, we can write the effective channel prediction from transmitter n to receiver m at time k as

$$\hat{h}^{(n,m)}[\ell|k] = |g_{n,m}|e^{j\hat{\phi}^{(n,m)}[\ell|k]} \quad (7)$$

since the channel amplitudes are assumed to be known. We denote the vector of channel predictions from all transmit nodes to receive node m as $\hat{\mathbf{h}}^{(m)}[\ell|k] \in \mathbb{C}^N$ for $\ell > k$.

3.1. Zero-Forcing Transmit Vector Calculation

Under our assumption that $M < N$, we can select the transmit vector $\mathbf{w}[\ell] \in \mathbb{C}^N$ to be orthogonal to $\hat{\mathbf{h}}^{(m)}[\ell|k]$ for all $m = 1, \dots, M$ and then use the remaining degrees of freedom in the transmit vector to maximize the received power at the intended receiver. The “zero-forcing” transmit vector is then

$$\mathbf{w}[\ell] = \alpha[\ell] \left[\mathbf{I} - \hat{\mathbf{H}}[\ell|k] \left(\hat{\mathbf{H}}^H[\ell|k] \hat{\mathbf{H}}[\ell|k] \right)^{-1} \hat{\mathbf{H}}^H[\ell|k] \right] \hat{\mathbf{h}}^{(0)}[\ell|k] \quad (8)$$

$$= \alpha[\ell] \hat{\mathbf{P}}[\ell|k] \hat{\mathbf{h}}^{(0)}[\ell|k] \quad (9)$$

where $\hat{\mathbf{H}}[\ell|k] = \left[\hat{\mathbf{h}}^{(1)}[\ell|k], \dots, \hat{\mathbf{h}}^{(M)}[\ell|k] \right] \in \mathbb{C}^{N \times M}$ and $\alpha[\ell]$ is a scale factor selected to satisfy a per-node or total power constraint.

4. PERFORMANCE ANALYSIS

This section provides analytical approximations and bounds on the expected performance of the receiver-coordinated technique under a total power constraint such that $\mathbf{w}^H[\ell]\mathbf{w}[\ell] = \beta$. These analytical predictions are verified via Monte-Carlo simulation in Section 5.

4.1. Expected Power at the Intended Receive Node

Distributed beamforming is quite robust to channel prediction errors, e.g., better than 90% of the ideal SNR gain is achieved even with 30° phase errors [6]. The zero-forcing solution inherits this robustness in terms of the power delivered to the intended receiver: errors in the spatial responses to the protected receivers change the geometry of the protected subspace, but this has a relatively small effect on the inner product of the zero-forcing solution and the desired spatial response. Thus, to first order, we can model the received power at the desired receiver as the beamforming power (possibly reduced due to channel estimation errors), attenuated by the loss due to zero-forcing, which is given by $\eta_{ZF} = \frac{\|\mathbf{P}\mathbf{h}^{(0)}\|^2}{\|\mathbf{h}^{(0)}\|^2}$ where \mathbf{P} denotes the projection orthogonal to the protected space. The beamforming power scales as the number of nodes N , while the zero-forcing loss increases with the number of protected nodes M . If the spatial responses were well-modeled as random, then results from the CDMA literature can be used to estimate this loss by $1 - \frac{M}{N}$ for large N , which would predict power scaling as $N - M$. However, the spatial responses are far more structured for typical node geometries, and explicit computation is required for accurate estimation of η_{ZF} .

4.2. Expected Power at a Protected Receive Node

We denote the received power at protected receive node m at time k as $\rho^{(m)}[\ell|k]$. The average received power is then

$$\begin{aligned} \mathbb{E}\{\rho^{(m)}[\ell|k]\} &= \mathbb{E}\{\|\mathbf{w}^H[\ell]\hat{\mathbf{h}}^{(m)}[\ell|k]\|^2\} \\ &= \mathbb{E}\{\|\mathbf{w}^H[\ell](\hat{\mathbf{h}}^{(m)}[\ell|k] - \tilde{\mathbf{h}}^{(m)}[\ell|k])\|^2\} \\ &= \mathbb{E}\{\|\mathbf{w}^H[\ell]\tilde{\mathbf{h}}^{(m)}[\ell|k]\|^2\} \end{aligned}$$

since $\mathbf{w}^H[k]\hat{\mathbf{h}}^{(m)}[\ell|k] = 0$ and where the channel prediction error vector at receive node m is defined as $\tilde{\mathbf{h}}^{(m)}[\ell|k] = \hat{\mathbf{h}}^{(m)}[\ell|k] - \hat{\mathbf{h}}^{(m)}[k]$. Given a channel phase prediction error $\tilde{\phi}^{(n,m)}[\ell|k] = \hat{\phi}^{(n,m)}[\ell|k] - \phi^{(n,m)}[k]$ small enough such that small angle approximations are sufficiently accurate, we can relate the real phase prediction error and the complex channel prediction error as

$$\tilde{h}^{(n,m)}[\ell|k] \approx jh^{(n,m)}[k]\tilde{\phi}^{(n,m)}[\ell|k] = j|g_{n,m}|e^{j\phi^{(n,m)}[k]}\tilde{\phi}^{(n,m)}[\ell|k].$$

We assume (i) the channel amplitudes are known, (ii) the channel phases $\phi^{(n,m)}[k]$ are mutually independent uniformly distributed on $[-\pi, \pi)$, (iii) the channel phase prediction errors are mutually independent zero-mean Gaussian distributed with variance $\sigma_{n,m}^2[\ell|k]$, and (iv) the channel phase prediction errors are independent of the channel phases. Under these assumptions, $\tilde{h}^{(n,m)}[\ell|k]$ are circularly symmetric independent zero mean Gaussian random variables with covariance $\mathbf{S}^{(m)}[\ell|k] = \mathbb{E}\{\tilde{\mathbf{h}}^{(m)}[\ell|k](\tilde{\mathbf{h}}^{(m)}[\ell|k])^H\} = \text{diag}(|g_{1,m}|^2\sigma_{1,m}^2[\ell|k], \dots, |g_{N,m}|^2\sigma_{N,m}^2[\ell|k])$. Note $\mathbf{S}^{(m)}[\ell|k]$ can be obtained directly from the local Kalman filter state prediction covariance matrix $\Sigma^{(m)}[\ell|k]$ and the known channel amplitudes.

If we further assume the channel prediction errors are sufficiently small such that $\mathbf{w}[\ell]$ is approximately independent of the channel prediction errors, then we can condition on the transmit vector to write

$$\mathbb{E}\{\rho^{(m)}[\ell|k] | \mathbf{w}[k]\} = \mathbf{w}^H[\ell]\mathbf{S}^{(m)}[\ell|k]\mathbf{w}[\ell]$$

Under a total power constraint $\mathbf{w}^H[\ell]\mathbf{w}[\ell] = \beta$, this leads to unconditional upper and lower bounds on the power at protected receive node m as

$$\beta \min_n \gamma_n[\ell|k] \leq \mathbb{E}\{\rho^{(m)}[\ell|k]\} \leq \beta \max_n \gamma_n[\ell|k] \quad (10)$$

with $\gamma_n[\ell|k] = |g_{n,m}|^2\sigma_{n,m}^2[\ell|k]$. These upper and lower bounds coincide when the channels from the transmit cluster to receive node m have identical magnitudes and the channel phase prediction errors are identically distributed.

Note that the bounds in (10) are not functions of the number of transmit nodes N . The expected null depth only depends on the total power emitted by the transmit cluster, the channel magnitudes, and the variances of the phase prediction errors. As an example of the sensitivity of nullforming to channel prediction error, if $|g_{n,m}|^2 \equiv 1$, $\beta = 1$, and the channel prediction errors are i.i.d. with zero mean and $\sigma_{n,m}[\ell|k] = \frac{2\pi \cdot 3}{360}$ (corresponding to 3 degree RMS channel prediction errors), we can compute the expected received power at a protected receiver to be -25.62 dB. With 30 degree RMS channel prediction errors, the null depth becomes only -5.62 dB.

5. NUMERICAL RESULTS

This section presents a numerical example of the receiver-coordinated distributed nullforming technique described in this paper. $N = 4$ transmit nodes are placed at (x, y) coordinates (1,0), (0,1), (-1,0),

(0,-1) with all units in meters. The intended receive node is placed at (50, 0) and there are two protected receiver nodes placed at $(50 \cos(\pi/8), \pm 50 \sin(\pi/8))$. The carrier frequency was set to $f_c = 900$ MHz and the receiver-coordinated protocol used a measurement interval of $T_m = 0.5$ seconds. The measurement epoch was set to the first 10 ms of each 500 ms measurement interval, corresponding to a 2% measurement overhead. The feedback latency was set to one full measurement interval, i.e. the state estimate feedback is used to generate predictions in the second subsequent distributed transmission interval (as illustrated in Figure 2). The oscillator parameters were derived from the Allan variance measurements on the Rakon RPFO45 oven-controlled oscillator datasheet and scaled to 900MHz to arrive at the values $p_t^{(n)} = p_r^{(m)} = 3 \times 10^{-4}$ seconds and $q_t^{(n)} = q_r^{(m)} = 1 \times 10^{-2}$ Hertz. The oscillators initial frequency offsets were uniformly distributed over ± 0.04 ppm. A single-path propagation model was used with channel amplitudes calculated as $|g_{n,m}| = \frac{50}{d_{n,m}}$ where $d_{n,m}$ is the distance between transmit node n and receive mode m in meters. The nominal phase offset measurement noise variance was set to $r_{n,m} = \frac{((5/360)2\pi)^2}{|g_{n,m}|^2}$ which corresponds to a standard deviation of 5 degrees at a nominal range of 50 meters. The total transmit power was set to $\mathbf{w}^H[\ell]\mathbf{w}[\ell] = 1$.

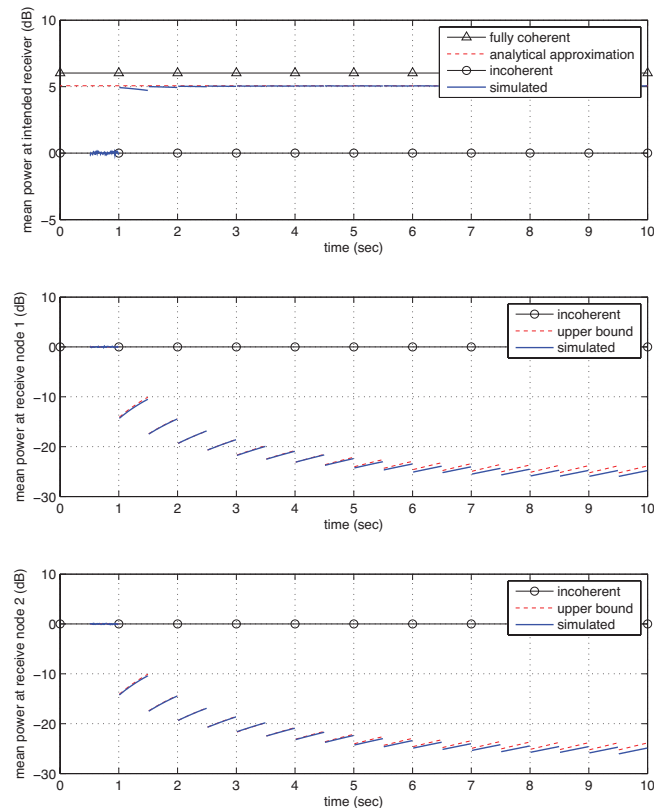


Fig. 3. Received power simulation for a system with $N = 4$ transmit nodes and $M = 2$ protected receive nodes. The upper bound on the received power at the protected receive nodes is from (10).

Figure 3 shows the results of a Monte-Carlo simulation with 1000 iterations. In each iteration, new realizations of the initial frequency offsets, clock process noises, and measurement noises were generated. Distributed transmission begins at $t = .510$ seconds, cor-

responding to the start of the first distributed transmission epoch in which the phase predictions from the feedback were available. The margin between the power at the intended receive node and incoherent reception is approximately 5 dB. This is almost exactly as predicted by an analysis of ideal zero-forcing: ideal beamforming with $N = 4$ leads to a gain of 6 dB, while the zero-forcing loss η_{ZF} for the given geometry is found to be -0.96 dB, showing that channel estimation errors have minimal effect on the power at the intended receiver. While the nullforming performance is more sensitive to estimation errors, we still do achieve deep nulls at the protected receivers after the Kalman filter startup transient: the margin between the power at the intended receive node and the protected receive node is between 25 and 30 dB, even though all receive nodes are at the same range from the center of the transmit cluster. The nulling performance is better at the start of each distributed transmission interval but degrades somewhat by the end of the distributed transmission interval as the state predictions become more stale. This can be ameliorated to some extent by shortening the measurement interval and/or reducing the feedback latency.

6. CONCLUSION

This paper demonstrates that receiver-coordinated coherent cooperative communication can provide effective beamforming and nullforming performance, using a standard zero-forcing solution with suboptimal local state tracking, with low measurement overhead and despite significant feedback latency. The residual power at the nulls depends on the channel estimation error, and for the parameters considered here, null depths in excess of 20 dB are achieved relative to the incoherent power seen at a typical location. While clock drifts are the main impairment considered here, our state space approach can model channel variations due to node motion as well, and it is of interest to quantify system performance in typical mobility regimes. Another key issue is to explore the effect of an imperfect feedback channel. Preliminary results indicate that the degradation due to loss of feedback packets is graceful, but a more detailed investigation is required. While our zero-forcing formulation is based on an average power constraint across the distributed transmit array, it is also of interest to implement beamforming and nullforming subject to per-transmitter peak power constraints. Finally, it is of interest to quantify the performance loss incurred, with respect to optimal fully-joint state tracking, of the suboptimal local state tracking approach proposed in this paper.

7. REFERENCES

- [1] R. Mudumbai, D.R. Brown III, U. Madhow, and H.V. Poor, "Distributed transmit beamforming: Challenges and recent progress," *IEEE Comm. Mag.*, vol. 47, no. 2, pp. 102–110, Feb. 2009.
- [2] K. Zarifi, S. Affes, and A. Ghayeb, "Collaborative null-steering beamforming for uniformly distributed wireless sensor networks," *IEEE Trans. on Signal Processing*, vol. 58, no. 3, pp. 1889–1903, Mar. 2010.
- [3] D.R. Brown III and U. Madhow, "Receiver-coordinated distributed transmit nullforming with channel state uncertainty," in *Conf. Inf. Sciences and Systems (CISS2012)*, Mar. 2012, to appear.
- [4] R. Preuss and D.R. Brown III, "Two-way synchronization for coordinated multi-cell retrodirective downlink beamforming," *IEEE Trans. Signal Proc.*, vol. 59, no. 11, pp. 5415–27, Nov. 2011.
- [5] L. Galleani, "A tutorial on the 2-state model of the atomic clock noise," *Metrologia*, vol. 45, no. 6, pp. S175–S182, Dec. 2008.
- [6] R. Mudumbai, G. Barriac, and U. Madhow, "On the feasibility of distributed beamforming in wireless networks," *IEEE Trans. on Wireless Communications*, vol. 6, no. 5, pp. 1754–1763, May 2007.